0013-7227/08/$15.00/0
Printed in U.S.A.

Endocrinology 149(6):2888–2898

doi: 10.1210/en.2007-1763

Intracellular Proadrenomedullin-Derived Peptides Decorate the Microtubules and Contribute to Cytoskeleton Function

Dan L. Sackett, Laurent Ozbun, Enrique Zudaire, Lisa Wessner, John M. Chirgwin, Frank Cuttitta, and Alfredo Martínez

Laboratory of Integrative and Medical Biophysics (D.L.S.), National Institute of Child Health and Human Development, and Cell and Cancer Biology Branch (L.O.), National Cancer Institute, Bethesda, Maryland 20892; Angiogenesis Core Facility (E.Z., F.C.), National Cancer Institute, Gaithersburg, Maryland 20877; Department of Medicine (L.W., J.M.C.), University of Virginia, Charlottesville, Virginia 22908; and Department of Cellular, Molecular, and Developmental Neurobiology (A.M.), Instituto Cajal, Consejo Superior de Investigaciones Científicas, 28002 Madrid, Spain

Adrenomedullin (AM) and proadrenomedullin N-terminal 20 peptide (PAMP) are secretory hormones, but it is not unusual to find them in intracellular compartments. Using yeast-2 hybrid technology, we found interactions between AM and several microtubule-associated proteins (MAPs), and between PAMP and tubulin. Expression of fluorescent-tagged AM and PAMP as well as immunofluorescence for the native peptides showed a complete decoration of the microtubules and colocalization with other MAPs. PAMP, but not AM, bound to tubulin *in vitro* and destabilized tubulin polymerization. Down-regulation of the gene coding for both AM and PAMP through small interfering RNA technology resulted in morphological changes, microtubule stabilization, increase in posttranslational modifications of tubulin such as acetylation and detyrosination, reduction in cell motility, and partial arrest at the G2 phase of the cell cycle, when compared with cells transfected with the same vector carrying a scrambled sequence. These results show that PAMP is a novel MAP, whereas AM may be exerting more subtle effects in regulating cytoskeleton function. (*Endocrinology* 149: 2888–2898, 2008)

THE PROADRENOMEDULLIN (proAM) precursor molecule is the source of two biologically active peptides, adrenomedullin (AM), which is a 52-amino acid long peptide hormone that contains an intramolecular disulfide bond, and proadrenomedullin N-terminal 20 peptide (PAMP). Both molecules are amidated at their carboxy terminus, and are expressed by a wide variety of tissues and cell types throughout vertebrate species, in which they play a range of physiological functions. These regulatory roles include vasodilatation, bronchodilatation, renal homeostasis, hormonal regulation, neurotransmission, antimicrobial activity, growth, and angiogenesis, among others (for a complete review, see Ref. 1). In addition, they are involved in the physiopathology of several relevant diseases such as hypertension, cardiovascular diseases, cancer, and diabetes (2, 3).

The intracellular distribution of AM and PAMP in classical endocrine organs follows the expected pattern for a secretory peptide, accumulating in the lumen of the secretory granules, as shown in the F cells of the endocrine pancreas (4, 5), the anterior pituitary (6), the adrenals (7), cells of the diffuse endocrine system in the gut (8), the juxtaglomerular complex of the kidney (9), or the glomus cells of the carotid body (10).

First Published Online March 6, 2008

Abbreviations: AM, Adrenomedullin; CHO, Chinese hamster ovary; CKAP1, cytoskeleton-associated protein 1; DAPI, 4′,6-diamidino-2-phenylindole; GAPDH, glyceraldehyde-3-phosphate dehydrogenase; MAP, microtubule-associated protein; PAMP, proadrenomedullin N-terminal 20 peptide; proAM, proadrenomedullin; siRNA, small interfering RNA.

***Endocrinology* is published monthly by The Endocrine Society (http://www.endo-society.org), the foremost professional society serving the endocrine community.**

In contrast, the few ultrastructural studies performed in nonendocrine organs show a different distribution. For instance, most of the deposits associated with AM immunoreactivity encountered in neurons are found in the proximity of the cytoskeleton or in the cytoplasmic side of mitochondrial and nuclear membranes, rather than in the synaptic vesicles (11). In ciliated cells of the bronchial epithelium, AM immunoreactivity accumulates in the apical cytoplasm in close proximity to the ciliary roots (12). This localization may represent an active secretion to the lumen through a nonregulated secretory pathway (12), but it could also suggest a specific intracellular function. It is also interesting that in specific areas of the rat brain (olfactory bulb and caudate putamen), AM immunoreactivity is restricted to the cell nucleus, whereas in the rest of the brain, AM is always found in the cytoplasm (11), thus revealing a tightly regulated subcellular distribution.

Several classical peptide hormones such as insulin, epidermal growth factor, platelet derived growth factor, nerve growth factor, and prolactin, among others, play intracellular roles as well (13). Given their wide range of activities, it would not be surprising if AM and PAMP were another example of this growing set of intracellularly active hormones. To explore this possibility, we decided to perform a yeast-2 hybrid screening using AM or PAMP as the bait, so as to identify molecular partners for these molecules and determine potential intracellular functions of these peptides. This analysis identified several microtubule-associated proteins (MAPs) as binding partners of AM, and tubulin as a binding partner for PAMP. Here, we present experimental

evidence showing that AM and PAMP decorate microtubules in cells from different origins. In addition, down-regulation of proAM expression by small interfering RNA (siRNA) knockdown or gene knockout technology has a profound effect on cytoskeleton morphology, cell cycle, and migration capabilities in the affected cells.

Materials and Methods

Yeast-2 hybrid

The reading frame for the human 52-amino acid AM peptide followed by the amidation motif was cloned into the *Nco*I-*Bam*HI sites of the bait vector pGBKT7 (Clontech, Palo Alto, CA) using as primers: sense 5′-GCC ATG GAG TAC CGC CAG AGC ATG AAC AAC-3′ and antisense 5′-GGA TCC GGA GCG CCG GCG CCG GCG GCC GTA GCC CTG-3′. The reading frame for human PAMP, containing the amidation motif, was cloned into the *Kpn*I-*Sma*I sites of the bait vector pLexA-N (Dualsystems, Zürich, Switzerland) using as primers: sense GGT ACC GCT CGG TTG GAT GTC GCG TCG and antisense CCC GGG CGC CTC TTC CCA CGA CTC AGA GC. Cloning fidelity was ensured by sequencing. The bait plasmid was transfected into yeast strain AH109 containing an adult human brain library using the Yeastmaker Transformation system (BD Biosciences, San Jose, CA, Clontech), and interacting clones identified by the ability to grow on minimal SD agar medium lacking adenine, histidine, leucine, and tryptophan (quadruple synthetic dropout selection plates). Prey plasmids were recovered and retransformed into AH109 with the bait or GAL4 DNA binding domain alone to verify interactions by β-galactosidase filter lift assays and by β-galactosidase liquid assays. The identity of interacting clones was determined by DNA sequencing.

Generation of vectors expressing AM, PAMP, and cytoskeleton-associated protein 1 (CKAP1) fused to fluorescent proteins

The reading frame for human AM was inserted into the *Eco*RI-*Bam*HI site of the red fluorescent protein carrying vector pHcRed1-C1 (Clontech) using as primers: sense 5′-GAA TTC TTA CCG CCA GAG CAT GAA CAA C-3′ and antisense 5′-GGA TCC GGA GCG CCG GCG CCG GCG GCC GTA GCC CTG-3′. This plasmid was named pRed-AM. The reading frame for human PAMP was inserted into the *Eco*RI-*Bam*HI site of the green fluorescent protein carrying vector pEGFP-C1 (Clontech) using as primers: sense 5′-GAA TTC TGC TCG GTT GGA TGT CGC GTC G-3′ and antisense 5′-GGA TCC CCT CTT CCC ACG ACT CAG AGC-3′. This vector was named pGreen-PAMP. At the same time, the reading frame for human CKAP1 was inserted into the green fluorescent protein carrying vector pEGFP-C3 (Clontech) with primers: sense 5′-GAA TTC TAC GAG GAG GAG CGG GCT C-3′ and antisense 5′-GGA TCC TCA TAT CTC GTC CAA CCC-3′. This vector was named pGreen-CKAP. All clones were analyzed by sequencing.

Microtubule binding protein spin-down assay

To investigate whether AM and PAMP are microtubule binding proteins (MAPs), synthetic human AM or PAMP (Phoenix Pharmaceuticals, Inc., Mountain View, CA) at a final concentration of 2.0 mM was incubated with taxol-stabilized microtubules for 30 min at room temperature, following the indications of the Microtubule Binding Protein Spin-Down Assay Kit (Cytoskeleton, Denver, CO). Microtubules were pelleted by centrifugation at 100,000 × *g* for 40 min at room temperature. Aliquots of both the pellets and supernatants were mixed with loading buffer and analyzed by Western blotting with the AM or PAMP antibody as described below. The immunoreactive bands were quantified by densitometry.

Microtubule polymerization assay

The effects of AM and PAMP on tubulin polymerization were investigated using the high-throughput screening-tubulin polymerization assay kit (Cytoskeleton). Briefly, bovine brain tubulin (400 μg/sample) in the presence and absence of synthetic human AM (1 μM to 2 mM), synthetic human PAMP (1 nM to 1 μM), or 200 μM paclitaxel (Cytoskeleton) was incubated in PEM buffer [80 mM PIPES, 1 mM EGTA, 1 mM $MgCl_2$ (pH 6.8)] containing 1.0 mM GTP (G-PEM) at 37 C, and the degree of polymerization over time was measured in a spectrophotometer (Fluostar Optima; BMG Labtechnologies, Offenburg, Germany) at 340 nm.

Construction of siRNA vectors against proAM

Five target sequences within the human proAM mRNA sequence (GenBank NM_01124) were chosen based upon position in the mRNA sequence as well as GC content within the 40–60% range. They were identified with siRNA target finder software available on-line at www.ambion.com, according to the selection criteria published at www.ambion.com/techlib/tb/tb_506.html. Primer pairs were made and the sequences amplified using Ambion's Silencer Express siRNA Expression Cassette Kit (Ambion, Inc., Austin, TX). The primer pairs introduce an RNA polymerase initiation site and 5′ *Eco*RI and 3′ *Hin*dIII restriction sites for direct cloning into the pSEC vectors. The five amplicons were transcribed into RNA *in vitro* and tested by transient transfection of Chinese hamster ovary (CHO) cells cotransfected with pFLAG-AM (14) followed by RT-PCR. The two sequences showing a higher degree of silencing were inserted into the human U6 promoter-driven pSEC vector (Ambion) by *Eco*RI and *Hin*dIII digestion and ligation. The target sequences for these siRNAs are AAG GAA TAG TCG CGC AAG CAT (this vector was called pSEC-AM735), and AAG CTG GCA CAC CAG ATC TAC (pSEC-AM511). Vectors containing scrambled versions of the same sequences were used as controls. The sequences were AAG ACG GAC GGC AAG TCC TAC (pSEC-AM735scr) and AAG GCG CCA CTC GCC CAA ATA AT (pSEC-AM511scr).

Cell lines, transfections, and confocal microscopy

Cell lines COS7 (monkey kidney), A549 (human lung adenocarcinoma), CHO, and PC12 (rat pheochromocytoma) were obtained from the American Type Culture Collection (Manassas, VA). The human neuroblastoma cell lines BE2 and KCNR were a generous gift from Dr. Carol Thiele (National Cancer Institute, Bethesda, MD). The rat hypothalamic immortalized cell line H32 was a generous gift from Dr. Greti Aguilera (National Institute of Child Health and Human Development, Bethesda, MD) (15). COS7 and A549 cells were transfected with the indicated plasmids using FuGENE 6 transfection reagent (Roche, Basel, Switzerland). Stable transfectants were selected by adding to the medium 800 μg/ml Geneticin (Invitrogen, Carlsbad, CA), and the levels of AM mRNA and protein were characterized by real-time PCR and Western blotting, respectively, as reported (10, 16).

Transfected cells were seeded into glass slides and eventually fixed in 10% formalin for 10 min. Cells destined for immunocytochemical procedures were permeabilized with 0.1% Triton X-100, blocked with 3% normal goat serum, and exposed to primary antibodies overnight at 4 C. Primary antibodies include mouse monoclonal anti-α tubulin (clone DM1A; Sigma-Aldrich, St. Louis, MO) and rabbit anti-de-tyrosinated α-tubulin (glu-tubulin; CHEMICON International, Inc., Temecula, CA). The following day, a mixture of Bodipy-phallacidin (Molecular Probes, Inc., Eugene, OR) and Texas-red goat antirabbit or antimouse IgGs (Molecular Probes) was applied to the cells for 1 h, followed by 4′,6-diamidino-2-phenylindole (DAPI) (Molecular Probes) as a nuclear counterstain. Unmodified cells were stained with antibodies against α-tubulin (as previously described) and rabbit anti-AM or anti-PAMP antibodies prepared in house (5, 9). Slides were analyzed with a Zeiss Laser Scanning Microscope 510 (Carl Zeiss, Inc., Thornwood, NY), equipped with four lasers. Microtubule depolymerization was induced by exposure to cold temperature (4 C) for 30 min or by addition of 1×10^{-5} M nocodazole (Sigma-Aldrich).

Heterozygote AM-null mice (Fernández, A. P., J. Serrano, L. Tessarollo, F. Cuttitta, and A. Martínez, manuscript in preparation) were crossed, and pregnant females were killed at d 12. Mouse embryo fibroblasts were obtained by disaggregating embryo tissue in DMEM medium containing 10% fetal bovine serum. After several passages, these cells were immortalized by exposure to the large T-antigen containing vector, pRSV-T. Cell lines were genotyped by PCR, and the phenotype was confirmed by RIA of the conditioned medium for AM.

Western blotting

Transfected COS7 cells were homogenized in lysis buffer [50 mM Tris/HCl (pH 7.5), 150 mM NaCl, 1% Triton X-100, 1% deoxycholate, 0.1% (wt/vol) NaN_3, 1 mM EGTA, 0.4 mM EDTA, 1 mM phenylmethylsulfonylfluoride, 0.2 mM Na_3VO_4, and protease inhibitor cocktail] and sonicated. Lysates were clarified by centrifugation at 15,000 × *g* for 10 min, and protein concentration was estimated in the supernatant using the bicinchoninic acid protein assay kit from Pierce (Rockford, IL). Equal amounts of total protein (25 μg) were loaded into 4–12% NuPage Bis-Tris gels (Invitrogen), electrophoresed in 2-(N-morpholino) ethanesulfonic acid buffer, and transferred to nitrocellulose membranes (Invitrogen). Detection of tubulin immunoreactivity was accomplished with antibodies against acetylated tubulin (Sigma-Aldrich), glu-tubulin, and α-tubulin (Sigma-Aldrich). A monoclonal antibody against glyceraldehyde-3-phosphate dehydrogenase (GAPDH) (CHEMICON) was used as a loading control. The enhanced chemiluminescence Advance Western Blotting Detection Kit from Amersham Biosciences, Inc. (Piscataway, NJ) was used to develop the blots.

RIA

The concentrations of AM found in conditioned media of test samples were determined using a commercially available RIA kit (Phoenix Pharmaceuticals). Samples (1 ml) were initially diluted in an equal volume of 0.1% alkali-treated casein in PBS (pH 7.4), and applied to prewashed reverse-phase Sep-Pak C-18 cartridges (Waters Corp., Milford, MA). The peptide fraction was eluted from the C18 matrix with 3 ml 80% isopropanol containing 0.125 N HCl and freeze-dried overnight. AM levels found in lyophilized extracts were then determined by RIA following the manufacturer's instructions.

Motility assays. Vascular endothelial growth factor (0.1 nM) was placed at the bottom of a ChemoTx chamber (NeuroProbe Inc., Gaithersburg, MD) as a chemotactic factor (17). The intermediate membrane was coated with 10 μg/ml fibronectin, and in the upper chamber, 5.0×10^5 cells were added. After a 4-h incubation at 37 C, the membrane was fixed and stained (Protocol Hema3; Biochemical Sciences Inc., Swedesboro, NJ). The cells trapped in the porous membrane were photographed through a ×25 microscope objective, and the number of cells per photographic field was counted.

Cell cycle analysis. Cells were trypsinized and resuspended in propidium iodide solution (DNAcon3 kit; DakoCytomation, Carpinteria, CA) for 1 h at 4 C, following the manufacturer's instructions. Cells were analyzed for DNA content by flow cytometry in a Becton Dickinson FACScan cytometer (Mansfield, MA), and cell cycle analysis was performed with ModFit LT 1.01 software (Becton Dickinson).

Results

Yeast-2 hybrid screening

We screened for proteins that interact with full-length AM or PAMP using the yeast-2 hybrid system. The fragments of the human *adm* gene coding for the mature peptides were cloned into the bait plasmids, and protein expression in yeast strain AH109 was determined by Western blot analysis (data not shown). Briefly, a pretransformed human brain matchmaker cDNA library in the MAT-α yeast strain Y187 was mated with the MAT-a yeast strain AH109 transformed with the bait constructs. *ADE2*, *HIS3*, and *LacZ* reporter genes are under the control of GAL4-dependent promoters. A functional interaction between the two hybrids after the mating process would be expected to produce Ade and His prototrophs and β-galactosidase activity. For AM, 14 potential candidates were isolated from the primary screen on QDO selection plates. These were then subjected to a second round of screening to eliminate false positives by growing the candidates on QDO selection plates containing the indicator substrate X-α-Gal (Fig. 1A) and by β-galactosidase liquid culture assay (Fig. 1B) to detect α-galactosidase and β-galactosidase activity, respectively. The cDNAs were extracted from the 12 of 14 positive candidates that formed blue colonies on QDO/X-α-galactosidase selection plates and showed significant β-galactosidase activity, and identified by DNA sequencing (Table 1). Several of the potential binding partners of AM thus identified had the common feature of being MAPs. These included MAP1A (three clones), a major component of the microtubules in mature neurons (18, 19), CKAP1, which is involved in tubulin folding (20), and RANBP9, a Ran binding protein that has been described in association with the centrosome (21, 22).

A similar process was performed for PAMP. From an initial set of 21 positive clones, 16 passed all the screening tests and were subjected to sequencing to identify the prey proteins (Table 2). These included two clones containing tubulin β-2A, a main component of the microtubules, and another two clones with the sequence for the kinesin heavy chain member 2 (Kif2), a motor protein involved in spindle assembly and axonal transport (23).

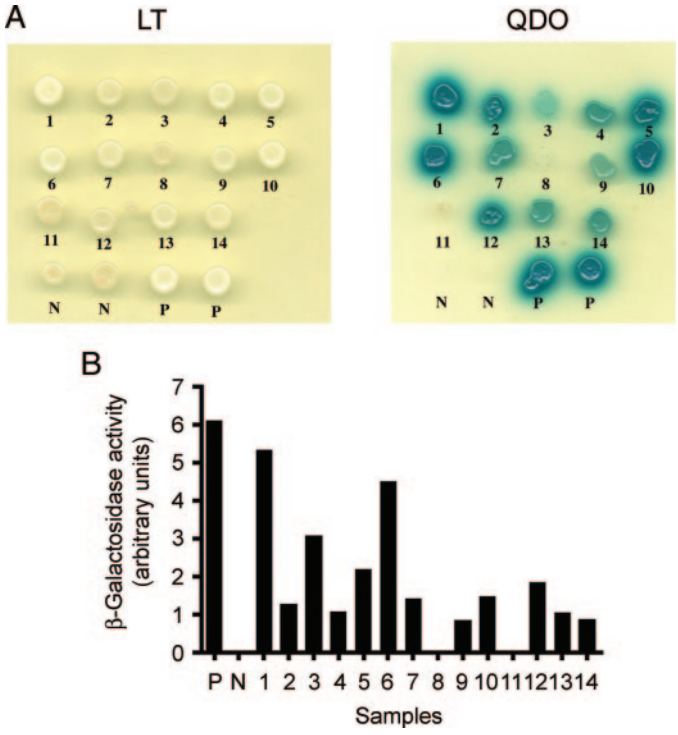

FIG. 1. Secondary screening of candidate yeast-2 hybrid colonies. A, Potential candidates were plated onto SD/-L/-T plates to verify the presence of the bait, and prey plasmids (*left panel*) and replica spotting of potential candidates from (LT) were also plated onto QDO plates (SD/-L/-T/-A/-H) containing X-α-Gal indicator substrate (*right panel*). *Blue* colonies are scored as positive candidates. *White* or no growth is considered to be false positives from the primary screen. One through 14 are candidate interactors. B, Quantification of β-galactosidase activity of candidate yeast colonies in liquid culture. Of the candidates, 12 (1–7, 9, 10, 12–14) produce significant β-galactosidase activity. Negative (N) control for β-galactosidase activity is yeast transformed with empty bait and prey vectors. Positive (P) control for β-galactosidase activity is yeast transformed with p53 prey and SV40 large T-antigen bait.

TABLE 1. Proteins identified by yeast-2 hybrid with AM as the bait

No. of clones	GenBank accession no.	Name	Function	Refs.
3	NM_002373	MAP1A	Regulates cytoskeleton in mature neurons	18
1	XM_056494	CKAP1	Tubulin folding factor	20
1	NM_005493	RANBP9	Centrosomal protein	21, 22
1	XM_045140	Prosaponin	Lipid interaction	
1	BC032626	TLH29	Cell cycle	
1	AF_508964	NTRK2	Noncatalytic form of surface receptor	
2	XM_165875	CDC2-related protein kinase 5	Cell cycle	
1	BC032691	FLJ10715	Unknown	
1	NM_006288	Thy-1 cell surface antigen	Unknown	

AM and PAMP are associated with microtubules in intact cells

To investigate whether AM and PAMP are found in microtubules, an AM-red fluorescent protein fusion expression vector was transfected into COS7 cells and the microtubules detected with an antitubulin antibody followed by a green fluorescent secondary IgG. Confocal images of these cells reveal a complete overlapping of the red and green fluorescence (Fig. 2, A–D) showing that AM fully decorates the microtubules. Double transfections with red-labeled AM and green-labeled CKAP1 also showed a complete colocalization along the length of the microtubules (Fig. 2, E–H).

To ensure that the presence of AM or PAMP in the microtubules was not an artifact of overexpressing the peptide at levels much higher than the ones found in unadulterated cells, several cell lines derived from brain tumors or an immortalized cell line obtained from rat hypothalamus (H32) were double stained with antibodies against tubulin and constitutive AM or PAMP. In all cases, AM, PAMP, and tubulin immunoreactivities overlapped on the microtubules (Fig. 2, I–L).

Exposure of cells to cold temperatures (4 C) or to nocodazole destabilizes their microtubules (22, 24). We hypothesized that if AM and PAMP are associated with microtubules, their cellular distribution must follow the same dynamics. As an example, COS7 cells transfected with pRed-AM lost the tubular aspect of the red fluorescence, which is observed under standard conditions (Fig. 3, A–C), when they were exposed to the cold (Fig. 3, D–F) or nocodazole (Fig. 3, G–I).

Microtubule binding and polymerization assays

To ascertain whether AM and PAMP are true MAPs, a microtubule spin-down assay was performed. AM did not get spun down by tubulin, but PAMP was. As expected for a MAP, the amount of PAMP in the supernatant fraction was higher in the absence of microtubules than in its presence, whereas the amount of peptide as detected by Western blotting increased in the pellet fraction of preparations containing microtubules (Fig. 4A). Interestingly, in the presence of microtubules, an immunoreactive band of about 60 kDa appeared. This band was never detected in the absence of microtubules or PAMP. Incubation with a set of MAPs resulted in a slight reduction in the intensity of the 60-kDa band, suggesting a competition between classical MAPs and PAMP. Because tubulin monomers have a molecular mass of 55 kDa, this band may represent the association of tubulin and PAMP.

To investigate whether AM and PAMP influence cytoskeleton function *in vitro*, microtubule polymerization assays in the presence and absence of AM or PAMP were performed. PAMP resulted in a significant delay in tubulin polymerization, whereas taxol, used as a control, markedly increased polymerization speed (Fig. 4B). This effect was observed even at very low concentrations of PAMP (down to 1 nM). Despite a large number of variations in the conditions of the assay (different concentrations of peptide, addition of MAPs to the tubulin preparation, increased concentrations of glycerol, *etc.*), we never saw any change in tubulin polymerization in the presence of AM (results not shown).

Identification of effective siRNA sequences for human AM down-regulation

Using Ambion's software tools, we selected five short sequences of the human proAM cDNA that complied with the restrictions imposed by the algorithm. These were 19 nucleotide-long oligonucleotides beginning at positions 17, 253, 511, 735, and 950 of the human cDNA (GenBank accession no. NM_01124). Double-stranded RNA containing these sequences was cotransfected into CHO cells together with plasmid pFLAG-AM, which overexpresses human AM mRNA. PCR analysis of total RNA from these cells revealed a strong

TABLE 2. Proteins identified by yeast-2 hybrid with PAMP as the bait

No. of clones	GenBank accession no.	Name	Function	Refs.
2	NM_001069.2	Tubulin β-2A	Cytoskeleton component	67
2	BC031828.2	Kinesin heavy chain member 2	Motor protein	23
3	AF144237.1	LOMP protein, LIM domain 7, LMO7	Focal adhesion	
4	NM_005680.1	TAF1B	Transcription initiation	
2	BC088371.1	EGF-like domain, variant 7	Notch4-like receptor	
1	NM_000386.2	Bleomycin hydrolase		
1	NM_004447.4	EPS8	EGF-R signaling	
1	NM_014941.1	MORC2	Meiosis inhibitor	

EGF, Epidermal growth factor; EGF-R, epidermal growth factor receptor.

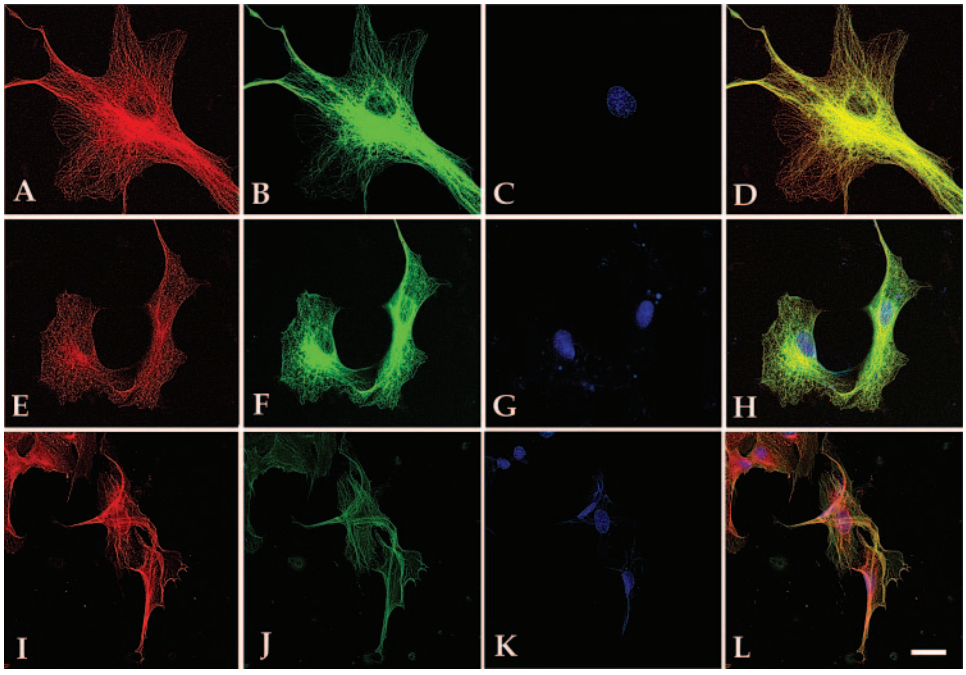

FIG. 2. AM and PAMP are associated with microtubules. Triple-color confocal microscopy of cell lines COS7 (A–H) and H32 (I–L). The *third column* (C, G, and K) shows nuclear counterstain with DAPI, and the *fourth column* (D, H, and L) is the combination of the previous images, with *yellow color* representing a complete overlapping of *red* and *green* signals. In the *first panel* (A–D), COS7 cells were transfected with pRed-AM (A) and stained with antibodies against tubulin, detected with a *green* fluorochrome (B). The *second panel* (E–H) shows a double transfection with pRed-AM (E) and pGreen-CKAP (F). The *third panel* shows double immunofluorescence for PAMP (I) and tubulin (J). *Bar*, 10 μm.

down-regulation of AM mRNA for all chosen sequences, being more potent for oligonucleotides 511 and 735 (Fig. 5A). These sequences were selected to generate siRNA expression vectors capable of sustaining stable expression. The human cell line A549 and the monkey cell line COS7 were stably transfected with vectors containing the siRNA sequence or a scrambled version as a negative control. We have shown that the monkey proAM cDNA is almost identical to its human counterpart (16), thus allowing the use of common reagents.

Real-time PCR analysis of proAM mRNA contents in the transfected cells showed a decrease of 54% in both cell lines with pSEC-AM735 (Fig. 5B), whereas pSEC-AM511 was less potent in reducing proAM levels (31% reduction, results not shown). To ensure that the decrease in mRNA was followed by a parallel decrease in protein, Western blot analyses were performed. In A549, a clear decrease in AM immunoreactivity was observed in cells transfected with pSEC-AM735 compared with the scrambled sequence (Fig. 5C). The pep-

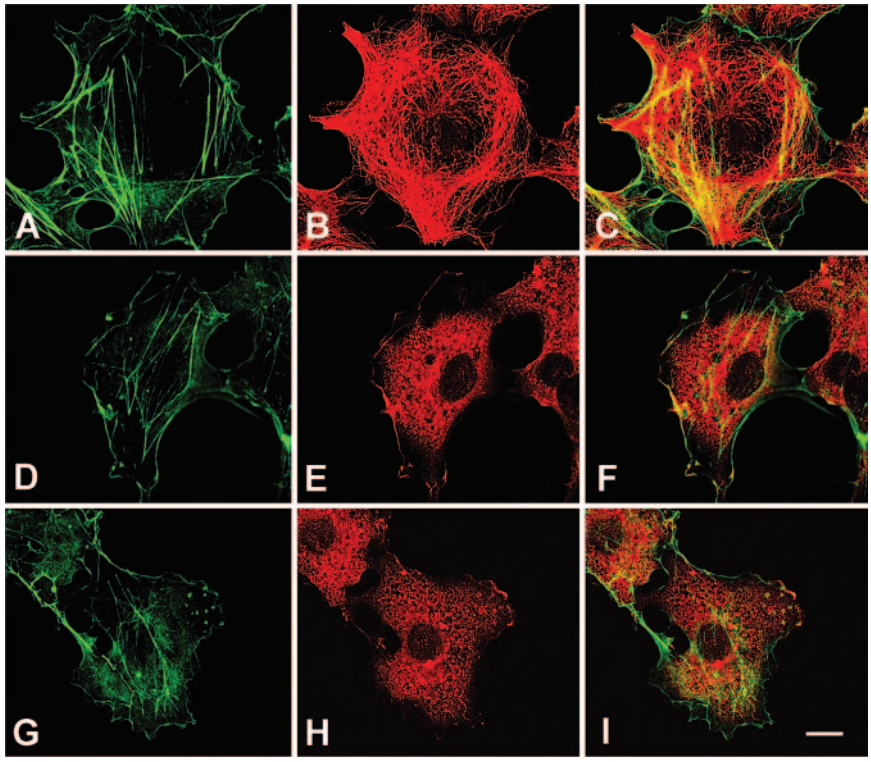

FIG. 3. Effects of microtubule destabilization on intracellular distribution of AM. COS7 cells were transfected with pRed-AM and exposed to control conditions (A–C), cold (4 C for 30 min) (D–F), or 10^{-5} M nocodazole (G–I). Cells were counterstained with Bodipy-phallacidin. *Bar*, 5 μm.

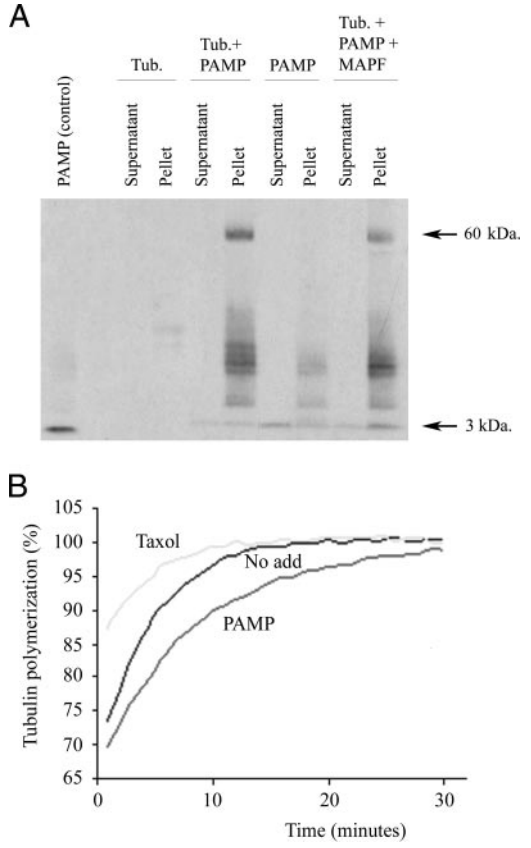

FIG. 4. Interactions of PAMP with tubulin as shown by spin down assay (A) and by tubulin polymerization assay (B). Taxol-stabilized microtubules (Tub) were incubated in the absence and presence of synthetic PAMP (with a molecular mass of 3 kDa) and/or microtubule-associated protein fraction (MAPF), centrifuged, and the supernatant was separated from the pellet. Both fractions were analyzed by Western blotting with an antibody against PAMP (A). For the tubulin polymerization assay (B), equal amounts of bovine brain tubulin in the presence and absence of PAMP or taxol were incubated at 37 C in 96-well plates, and the degree of polymerization was determined as a direct correlate of the absorption at 340 nm over time. The blot (A) and graph (B) are representative examples of three independent repeats. No add, No addition (control).

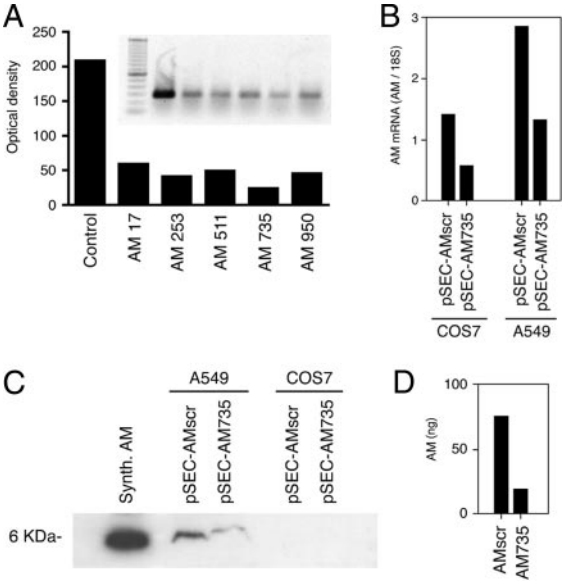

FIG. 5. A, Characterization of siRNAs for AM. Five double-stranded RNA sequences were transiently cotransfected with pFLAG-AM into CHO cells, and AM mRNA levels were analyzed by regular PCR. B, The more efficient sequence (AM735) and a scrambled version of it were cloned into pSEC, stable transfectants were generated in COS7 and A549 cells, and the AM mRNA levels in these transfected cells were quantified by real-time PCR. C, Protein extracts from the same cells were characterized by Western blotting with an antibody specific to AM. D, The supernatant of COS7 was also analyzed by RIA because the levels of AM were undetectable by Western blotting.

tide contents of COS7 were below the detection limit of the assay (Fig. 5C), so we performed a RIA for AM of the conditioned media to ensure that a significant decrease was taking place at the protein level (Fig. 5D).

Down-regulation of proAM expression changes cytoskeletal morphology

The consequences of proAM silencing in microtubule morphology and physiology were studied. The first change observed was a modification in cell shape in A549 cells transfected with the pSEC-AM735 vector. These cells showed a more pleomorphic aspect than their control counterparts transfected with the scrambled sequence, with long cell processes that gave these cells a more "spiky" look (Fig. 6, A and B). These changes were not so evident in COS7 cells (results not shown). These and the following results were similar when using either pSEC-AM735 or pSEC-AM511, although differences with controls were stronger with the former vector. Only results obtained with pSEC-AM735 are presented here for brevity sake.

When the stably transfected cells were labeled with an antitubulin antibody and analyzed by confocal microscopy, striking differences in cytoskeleton morphology were observed. Cells transfected with the scrambled sequence presented microtubules indistinguishable from the ones found in nontransfected cells. These microtubules were arranged in a star-like pattern emanating from the centrosome and reaching the cell periphery with a straight morphology (Fig. 6, C–E). In sharp contrast, cells expressing the siRNA for proAM had a higher number of microtubules, these were less organized, and they formed arch-like structures in the periphery of the cells (Fig. 6, F–H). This morphological pattern is similar to the one obtained with the administration of microtubule-stabilizing drugs, such as taxol (25).

In stabilized microtubules several posttranslational modifications occur. These include partial proteolysis of the carboxy-terminal tyrosine that exposes a glutamic acid residue, and acetylation at the amino end of the tubulin monomer (26, 27). Using a specific antibody against glu-tubulin, we found that cells expressing siRNA for proAM (Fig. 6, L–N) were more immunoreactive than the corresponding controls (Fig. 6, I–K), reinforcing the concept that proAM down-regulation induces microtubule stabilization.

Because cells expressing siRNA for proAM have a morphology consistent with microtubule hyperpolymerization, we hypothesized that their microtubules should be more resistant to cold than the ones in cells containing the scrambled sequence. After 30 min at 4 C, COS7 cells transfected

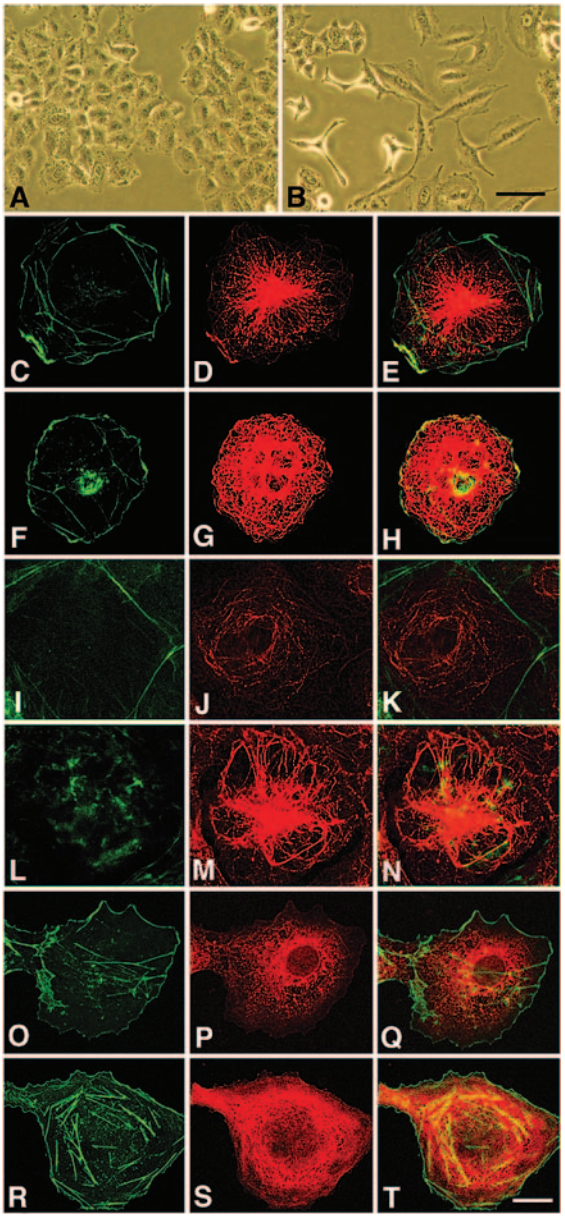

FIG. 6. Morphological effects of transfection with AM siRNA. A549 cells transfected with pSEC-AMscr (A) or pSEC-AM735 (B) present different morphological features under phase-contrast microscopy. *Bar*, 20 μm. Double-color confocal microscopy of COS7 cells (C–T) stained with Bodipy-phallacidin (*green*, C, F, I, L, O, and R) and an antibody against tubulin (D, G, P, and S) or glu-tubulin (J and M). The *third column* (E, H, K, N, Q, and T) is the combination of the previous images. Microtubules in COS7 cells transfected with pSEC-AMscr (C–E) have the typical radial pattern of this cell line, whereas the same cells transfected with pSEC-AM735 (F–H) contain more microtubular structures that curve at the cell surface and return back into the cell. When the same cells are stained with an antibody against polymerized tubulin (glu-tubulin), cells transfected with pSEC-AMscr (I–K) have only a few labeled microtubules, but cells transfected with pSEC-AM735 (L–N) display a complex system of curved microtubules. After exposure of these cells to a cold environment (4 C for 30 min), microtubules were completely depolymerized in pSEC-AMscr transfected cells (O–Q), whereas pSEC-AM735 containing cells maintained their cytoskeleton (R–T). *Bar*, 5 μm.

with pSEC-AMscr lost all of their microtubules (Fig. 6, O–Q), whereas cells transfected with pSEC-AM735 still had recognizable microtubular structures (Fig. 6, R–T).

To confirm that lower levels of proAM translate into a higher number of microtubules, we also analyzed immortalized cell lines of embryo fibroblasts obtained from wild-type and AM-heterozygous mice (Fig. 7). Wild-type cells displayed the characteristic morphology of regular microtubules (Fig. 7, A–D). In agreement with our AM knockdown experimental data, cells obtained from heterozygous AM embryos presented a much higher number of microtubules with the typical arches below the plasma membrane (Fig. 7, E–H).

Microtubule stabilization upon down-regulation of proAM levels was confirmed by Western blot analysis in COS7 cells. Immunoreactivity for two posttranslational modifications of tubulin related to microtubule stabilization (acetylated tubulin and glu-tubulin) was much higher in cells transfected with the siRNA for proAM than in the cells carrying the scrambled sequence (Fig. 8). The levels of total α-tubulin and GAPDH were the same between these two cell lines.

Down-regulation of AM changes microtubule-mediated functions

Microtubules are involved in a variety of cell behaviors, including cell cycle and motility (28, 29). To investigate whether proAM levels have an impact on microtubule-mediated functions, we analyzed these cell parameters in stably transfected cells.

Cell cycle analysis of COS7 cells transfected with pSEC-AM735 revealed a statistically significant G2 arrest and a concomitant decrease in the S phase when compared with cells transfected with the scrambled sequence (Table 3).

Cell migration was also examined with a chemotaxis assay. COS7 cells transfected with the siRNA cassette showed less migration efficiency than the scrambled control (Fig. 9).

Discussion

In this report we show that intracellular AM and PAMP decorate microtubules under both artificial and native conditions, and that PAMP decreases tubulin polymerization *in vitro*. In addition, proAM down-regulation by either siRNA technology or gene targeting results in morphological changes of the cytoskeleton and in modifications of microtubule-mediated functions. Thus, we can identify PAMP as a novel MAP involved in cytoskeleton homeostasis. Curiously, AM failed to modify specific assays for microtubule polymerization, indicating that AM is not a real MAP, although it might exert some functions through interaction with *bona fide* MAPs. We should point out that AM is well conserved through evolution, whereas PAMP has experienced wider sequence variations (30). It would be interesting to study whether all PAMP molecules, derived from different species, bind microtubules in the same fashion.

Several of the proteins that interact with AM and PAMP in the yeast-2 hybrid system were identified in several clones, confirming the strong interaction between both partners inside the yeasts.

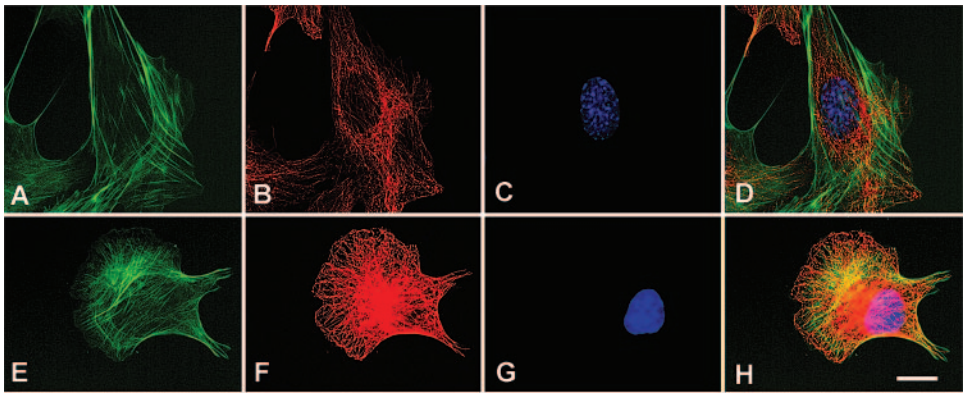

FIG. 7. Differences in cytoskeleton morphology between mouse embryo fibroblasts obtained from wild-type (A–D) and AM heterozygous (E–H) animals. Cells were grown in slides and stained with Bodipy-phallacidin (A and E), antitubulin detected in *red* (B and F), and DAPI (C and G). The *last column* (D and H) represents a composite of the previous images. *Bar*, 5 μm.

The core of the microtubules consists of a dynamic cylindrical polymer of tubulin. Microtubule dynamics involve the addition and loss of tubulin dimers from the ends of the microtubules through two different mechanisms: preferential addition at the "plus" end and loss at the "minus" end in the process of treadmilling, and preferential addition and loss at the plus end (compared with the minus end) in the process of dynamic stability (28, 31–33). Both processes can be active without altering the steady-state level of polymerized tubulin. However, microtubules can be modulated by MAPs, changes in tubulin isotypes, tubulin mutations, or microtubule-active drugs (24, 34, 35). These changes may alter the steady-state levels of polymerized tubulin as well as altering posttranslational modifications of tubulin (36, 37). The posttranslational modifications of tubulin that have been associated with stable microtubules include detyrosination of the carboxy terminus of α-tubulin (revealing the penultimate glutamic acid residue, and, therefore, often referred to as glu-tubulin), acetylation of lysine 40 in α-tubulin, as well as others (27, 38). These posttranslational changes have been demonstrated in the cells expressing lower levels of proAM. This observation is in agreement with the delay in tubulin polymerization induced by PAMP.

Many MAPs have been described. These are proteins that bind to the tubulin core and modulate the stability and/or functions of the microtubules. Specific MAPs can act as cellular motors (39, 40), tubulin-folding molecules (41), anchors to other cellular structures (42), or modulators of microtubule stability (43). The data presented in this report identify PAMP as a novel MAP involved in regulating microtubule assembly. In contrast, AM was identified as a peptide that decorates the microtubules but does not influence tubulin polymerization directly. Given that PAMP and AM are produced by the same gene, it is rather difficult to separate their individual contribution to cytoskeleton homeostasis through genetic techniques. The fact that PAMP is the only molecule of the two capable of modifying tubulin polymerization suggests a more relevant function for this peptide, but we cannot exclude a more subtle regulatory role for AM, possibly through interaction with other MAPs rather than directly on microtubule stability.

TABLE 3. Cell cycle parameters in transfected COS7 cells as measured by flow cytometry

	G1	G2	S
COS7 pSEC-AMscr	57.2 ± 1.0	11.9 ± 0.8	31.0 ± 0.3
COS7 pSEC-AM735	55.6 ± 1.5	16.0 ± 0.6	28.5 ± 1.0
P value	ns	0.002	0.01

Each point represents the mean and SD of three independent measurements. ns, Not statistically significant.

Our results are in agreement with previous observations that described the presence of AM immunoreactivity in areas rich in microtubules such as the dendritic processes in neurons (11) and the subciliary region in epithelial cells of the lung (12). In fact, if we compare immunohistochemical images for AM (11) and MAP1A (44) in pyramidal neurons of the rat brain, the patterns are identical. Our results also correlate well with a recent gene expression profile study comparing prostate tumor cells overexpressing AM with their wild-type counterparts. Some of the proteins whose expression was elevated in the cells with high levels of AM were cytoskeleton-related molecules (45). Less information is available for the distribution of PAMP, but both molecules derive from the same gene, and similar expression patterns are expected, although the existence of an alternative splicing mechanism that changes the ratio of expression has been described for this gene (46).

Genetic engineering to knockout or knockdown the gene of interest has been widely used to investigate the physiological contribution of particular gene products (47). Downregulation of proAM expression through siRNA technology or gene targeting results in microtubule hyperpolymerization, suggesting that AM and/or PAMP plays an important role in maintaining microtubule physiology. The morphology of the cytoskeleton in cells containing low levels of proAM is similar to the one observed after treatment with microtubule-stabilizing drugs such as taxol (48). This change in microtubule morphology translated into a modification of cell shape in A549 but not in COS7, indicating that cell morphology may be regulated by more parameters than just microtubule status. In addition, the cytoskeleton of cells with less proAM was more resistant to the cold than the controls, strengthening the concept that the lack of proAM induces microtubule hyperpolymerization.

In addition to cell shape (49), a number of other cell features require the intervention of the cytoskeleton, including regulation of the cell cycle and cell migration (28, 29). During the cell cycle, microtubules play a major role in mitosis in which the mitotic spindle separates the homologous chromatids into the resulting daughter cells (50–52). Drugs that

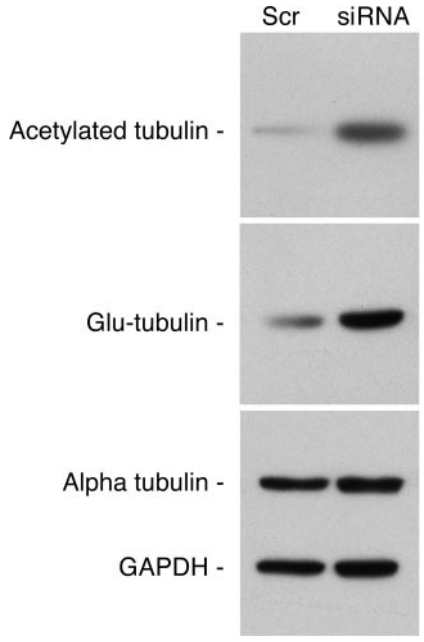

FIG. 8. Western blot analysis of COS7 cells transfected with either pSEC-AMscr (Scr) or pSEC-AM735 (siRNA). Immunoreactivity to acetylated tubulin and glu-tubulin is higher in cells expressing the AM siRNA. α-Tubulin and GAPDH immunoreactivities are shown as loading controls.

stabilize microtubules induce cell cycle arrest due to an inability to depolymerize the mitotic spindle (53, 54), among other effects. COS7 cells expressing lower proAM levels had a statistically significant increase in the number of cells found in G2. AM and PAMP have been previously identified as growth factors (55–57), but those effects were attributed to a paracrine/autocrine effect mediated through specific receptors at the cell surface. Although we cannot completely exclude the involvement of membrane receptors activated by the peptides, our present results indicate that AM and/or PAMP may also have an intracellular contribution to cell growth regulation by allowing cells to pass through mitosis unhindered. In a microarray analysis paper, Ma *et al.* (58) present evidence showing that up-regulation of E2F1 (a protein expressed during the G1 and S phases of the cell cycle and implicated in G1 to S transition) down-regulates AM levels in mouse fibroblasts. These data would suggest a decrease of proAM levels during the G1 and S phases of the cell cycle that, according to our results, may induce microtubule polymerization in preparation for spindle assembly.

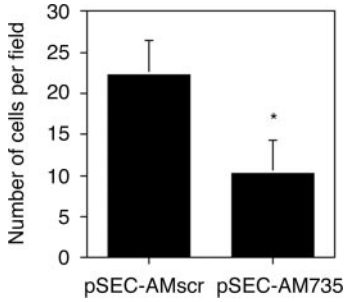

FIG. 9. Migration capabilities of cells with different levels of AM expression. COS7 cells transfected with pSEC-AMscr migrate at a higher rate than their counterparts transfected with pSEC-AM735. Each *bar* represents the mean and SD of six independent measurements. *, $P < 0.05$.

There is a link between microtubule polymerization status and cell motility, but this relationship may be complex. For instance, cells exposed to the microtubule-stabilizing agent paclitaxel (taxol) migrate faster than untreated controls, but when the same cells have been previously treated with ionizing radiation, paclitaxel-treated cells migrate at a slower rate than the corresponding controls (59). When tumor cells are treated with sublethal doses of paclitaxel, the surviving clones display more efficient chemotaxis than the original cells (60). On the other hand, microtubule hyperpolymerization produces the loss of neutrophil chemotaxis, but not random motility (61). We and others have shown that external addition of AM to cells in culture can result in either enhancement (14, 62) or reduction (63) of cell motility, depending on the cell type under scrutiny. In this study we show that reduction of proAM expression levels in COS7 cells results in a decrease in migration. As with the cell cycle regulation, we cannot exclude the fact that cells expressing less proAM secrete less peptide to the medium, and, thus, autocrine receptor activation would be lower.

In some animal models recapitulating human diseases, microtubule hyperpolymerization has been reported. This is the case of pressure-overload cardiac hypertrophy in which the cytoskeleton displays a marked hyperstabilization in the cardiomyocytes of treated cats (25). AM and PAMP have been described as protective peptides against heart remodeling, hypertrophy, and other cardiac dysfunctions (64). It would be interesting to investigate whether this protective function is mediated, at least in part, through the cytoskeleton.

Recent studies have shown that the phenotype of the proAM gene knockouts are very similar to those of the AM receptor CRLR/RAMP2 (65, 66), suggesting that circulating AM but not PAMP exerts potential function. Nevertheless, it has been shown that PAMP is a more potent angiogenic factor than AM (17), and here, we show a specific function for PAMP in cytoskeletal regulation. It may be that PAMP acts in a more local environment, as an autocrine or paracrine peptide (even at the intracellular level), whereas AM is more of a classical endocrine peptide hormone. More careful studies of the available knockout models may shed more light on this subject.

In conclusion, we have shown that AM and PAMP bind microtubules and decorate the cytoskeleton in a variety of cell types. PAMP reduces tubulin polymerization, whereas AM does not have any effect in this assay. Down-regulation of proAM results in cytoskeleton changes that modify cell behavior. Recognizing the intracellular functions of AM and/or PAMP may help to understand the impact of these molecules in normal physiology and in the diseases in which they seem to play a major role, such as cardiovascular and cerebrovascular dysfunctions, cancer, and diabetes (1).

Acknowledgments

We thank Dr. Robert Robey (National Cancer Institute, Bethesda, MD) for his assistance with flow cytometry, Dr. Carol Thiele (National Cancer Institute, Bethesda, MD) for the neuroblastoma cell lines, and Dr.

Greti Aguilera (National Institute of Child Health and Human Development, Bethesda, MD) for cell line H32.

Received December 19, 2007. Accepted February 25, 2008.

Address all correspondence and requests for reprints to: Alfredo Martínez, Ph.D., Department of Cellular, Molecular, and Developmental Neurobiology, Instituto Cajal, Consejo Superior de Investigaciones Científicas, 28002 Madrid, Spain. E-mail: amartinez@cajal.csic.es.

A.M. was supported by grants from the Spanish Ministry of Science and Education (BFU2004-02838, SAF2007-60010), and the Instituto de Salud Carlos III (RD06/0026/1001).

Disclosure Summary: The authors have nothing to disclose.

References

1. **López J, Martínez A** 2002 Cell and molecular biology of the multifunctional peptide, adrenomedullin. Int Rev Cytol 221:1–92
2. **Eto T, Samson WK** 2001 Adrenomedullin and proadrenomedullin N-terminal 20 peptide: vasodilatory peptides with multiple cardiovascular and endocrine actions. Trends Endocrinol Metab 12:91–93
3. **Zudaire E, Martinez A, Cuttitta F** 2003 Adrenomedullin and cancer. Regul Pept 112:175–183
4. **Lopez J, Cuesta N, Cuttitta F, Martinez A** 1999 Adrenomedullin in nonmammalian vertebrate pancreas: an immunocytochemical study. Gen Comp Endocrinol 115:309–322
5. **Martinez A, Weaver C, Lopez J, Bhathena SJ, Elsasser TH, Miller MJ, Moody TW, Unsworth EJ, Cuttitta F** 1996 Regulation of insulin secretion and blood glucose metabolism by adrenomedullin. Endocrinology 137:2626–2632
6. **Montuenga LM, Burrell MA, Garayoa M, Llopiz D, Vos M, Moody T, Garcia-Ros D, Martinez A, Villaro AC, Elsasser T, Cuttitta F** 2000 Expression of proadrenomedullin derived peptides in the mammalian pituitary: co-localization of follicle stimulating hormone and proadrenomedullin N-20 terminal peptide-like peptide in the same secretory granules of the gonadotropes. J Neuroendocrinol 12:607–617
7. **Yuchi H, Suganuma T, Sawaguchi A, Ide S, Kawano J, Aoki T, Kitamura K, Eto T** 2002 Cryofixation processing is an excellent method to improve the retention of adrenomedullin antigenicity. Histochem Cell Biol 118:259–265
8. **Tajima A, Osamura RY, Takekoshi S, Itoh Y, Sanno N, Mine T, Fujita T** 1999 Distribution of adrenomedullin (AM), proadrenomedullin N-terminal 20 peptide, and AM mRNA in the rat gastric mucosa by immunocytochemistry and in situ hybridization. Histochem Cell Biol 112:139–146
9. **Lopez J, Cuesta N, Martinez A, Montuenga L, Cuttitta F** 1999 Proadrenomedullin N-terminal 20 peptide (PAMP) immunoreactivity in vertebrate juxtaglomerular granular cells identified by both light and electron microscopy. Gen Comp Endocrinol 116:192–203
10. **Martinez A, Saldise L, Ramirez MJ, Belzunegui S, Zudaire E, Luquin MR, Cuttitta F** 2003 Adrenomedullin expression and function in the rat carotid body. J Endocrinol 176:95–102
11. **Serrano J, Uttenthal LO, Martinez A, Fernandez AP, Martinez de Velasco J, Alonso D, Bentura ML, Santacana M, Gallardo JR, Martinez-Murillo R, Cuttitta F, Rodrigo J** 2000 Distribution of adrenomedullin-like immunoreactivity in the rat central nervous system by light and electron microscopy. Brain Res 853:245–268
12. **Martinez A, Miller MJ, Unsworth EJ, Siegfried JM, Cuttitta F** 1995 Expression of adrenomedullin in normal human lung and in pulmonary tumors. Endocrinology 136:4099–4105
13. **Henderson JE** 1997 Nuclear targeting of secretory proteins. Mol Cell Endocrinol 129:1–5
14. **Martinez A, Vos M, Guedez L, Kaur G, Chen Z, Garayoa M, Pio R, Moody T, Stetler-Stevenson WG, Kleinman HK, Cuttitta F** 2002 The effects of adrenomedullin overexpression in breast tumor cells. J Natl Cancer Inst 94:1226–1237
15. **Volpi S, Rabadan-Diehl C, Cawley N, Aguilera G** 2002 Transcriptional regulation of the pituitary vasopressin V1b receptor involves a GAGA-binding protein. J Biol Chem 277:27829–27838
16. **Zudaire E, Martinez A, Ozbun LL, Cuttitta F** 2004 Characterization of adrenomedullin in non-human primates. Biochem Biophys Res Commun 321:859–869
17. **Martinez A, Zudaire E, Portal-Nunez S, Guedez L, Libutti SK, Stetler-Stevenson WG, Cuttitta F** 2004 Proadrenomedullin NH2-terminal 20 peptide is a potent angiogenic factor, and its inhibition results in reduction of tumor growth. Cancer Res 64:6489–6494
18. **Noiges R, Eichinger R, Kutschera W, Fischer I, Nemeth Z, Wiche G, Propst F** 2002 Microtubule-associated protein 1A (MAP1A) and MAP1B: light chains determine distinct functional properties. J Neurosci 22:2106–2114
19. **Halpain S, Dehmelt L** 2006 The MAP1 family of microtubule-associated proteins. Genome Biol 7:224
20. **Tian G, Lewis SA, Feierbach B, Stearns T, Rommelaere H, Ampe C, Cowan NJ** 1997 Tubulin subunits exist in an activated conformational state generated and maintained by protein cofactors. J Cell Biol 138:821–832
21. **Nakamura M, Masuda H, Horii J, Kuma K, Yokoyama N, Ohba T, Nishitani H, Miyata T, Tanaka M, Nishimoto T** 1998 When overexpressed, a novel centrosomal protein, RanBPM, causes ectopic microtubule nucleation similar to γ-tubulin. J Cell Biol 143:1041–1052
22. **Tang X, Zhang J, Cai Y, Miao S, Zong S, Koide SS, Wang L** 2004 Sperm membrane protein (hSMP-1) and RanBPM complex in the microtubule-organizing centre. J Mol Med 82:383–388
23. **Ganem NJ, Compton DA** 2004 The KinI kinesin Kif2a is required for bipolar spindle assembly through a functional relationship with MCAK. J Cell Biol 166:473–478
24. **Wilson L, Panda D, Jordan MA** 1999 Modulation of microtubule dynamics by drugs: a paradigm for the actions of cellular regulators. Cell Struct Funct 24:329–335
25. **Tagawa H, Wang N, Narishige T, Ingber DE, Zile MR, Cooper G** 1997 Cytoskeletal mechanics in pressure-overload cardiac hypertrophy. Circ Res 80:281–289.
26. **Kreitzer G, Liao G, Gundersen GG** 1999 Detyrosination of tubulin regulates the interaction of intermediate filaments with microtubules in vivo via a kinesin-dependent mechanism. Mol Biol Cell 10:1105–1118
27. **Westermann S, Weber K** 2003 Post-translational modifications regulate microtubule function. Nat Rev Mol Cell Biol 4:938–947
28. **Margolis RL, Wilson L** 1998 Microtubule treadmilling: what goes around comes around. Bioessays 20:830–836
29. **Thaler CD, Haimo LT** 1996 Microtubules and microtubule motors: mechanisms of regulation. Int Rev Cytol 164:269–327
30. **Martinez A, Bengoechea JA, Cuttitta F** 2006 Molecular evolution of proadrenomedullin N-terminal 20 peptide (PAMP): evidence for gene co-option. Endocrinology 147:3457–3461
31. **Valiron O, Caudron N, Job D** 2001 Microtubule dynamics. Cell Mol Life Sci 58:2069–2084
32. **Karsenti E, Nedelec F, Surrey T** 2006 Modelling microtubule patterns. Nat Cell Biol 8:1204–1211
33. **Morrison EE** 2007 Action and interactions at microtubule ends. Cell Mol Life Sci 64:307–317
34. **Cassimeris L, Spittle C** 2001 Regulation of microtubule-associated proteins. Int Rev Cytol 210:163–226
35. **Gupta S, Bhattacharyya B** 2003 Antimicrotubular drugs binding to vinca domain of tubulin. Mol Cell Biochem 253:41–47
36. **Bhattacharya R, Cabral F** 2004 A ubiquitous β-tubulin disrupts microtubule assembly and inhibits cell proliferation. Mol Biol Cell 15:3123–3131
37. **Poruchynsky MS, Kim JH, Nogales E, Annable T, Loganzo F, Greenberger LM, Sackett DL, Fojo T** 2004 Tumor cells resistant to a microtubule-depolymerizing hemiasterlin analogue, HTI-286, have mutations in α- or β-tubulin and increased microtubule stability. Biochemistry 43:13944–13954
38. **Gundersen GG, Cook TA** 1999 Microtubules and signal transduction. Curr Opin Cell Biol 11:81–94
39. **Li JY, Wu CF** 2003 Perspectives on the origin of microfilaments, microtubules, the relevant chaperonin system and cytoskeletal motors–a commentary on the spirochaete origin of flagella. Cell Res 13:219–227
40. **Vallee RB, Williams JC, Varma D, Barnhart LE** 2004 Dynein: an ancient motor protein involved in multiple modes of transport. J Neurobiol 58:189–200
41. **Szymanski D** 2002 Tubulin folding cofactors: half a dozen for a dimer. Curr Biol 12:R767–R769
42. **Hong Z, Geisler-Lee CJ, Zhang Z, Verma DP** 2003 Phragmoplastin dynamics: multiple forms, microtubule association and their roles in cell plate formation in plants. Plant Mol Biol 53:297–312
43. **Akhmanova A, Severin F** 2004 Thirteen is the lucky number for doublecortin. Dev Cell 7:5–6
44. **Cornea-Hebert V, Watkins KC, Roth BL, Kroeze WK, Gaudreau P, Leclerc N, Descarries L** 2002 Similar ultrastructural distribution of the 5-HT(2A) serotonin receptor and microtubule-associated protein MAP1A in cortical dendrites of adult rat. Neuroscience 113:23–35
45. **Gonzalez-Moreno O, Calvo A, Joshi BH, Abasolo I, Leland P, Wang Z, Montuenga L, Puri RK, Green JE** 2005 Gene expression profiling identifies IL-13 receptor α 2 chain as a therapeutic target in prostate tumor cells overexpressing adrenomedullin. Int J Cancer 114:870–878
46. **Martinez A, Hodge DL, Garayoa M, Young HA, Cuttitta F** 2001 Alternative splicing of the proadrenomedullin gene results in differential expression of gene products. J Mol Endocrinol 27:31–41
47. **Sung YH, Song J, Lee HW** 2004 Functional genomics approach using mice. J Biochem Mol Biol 37:122–132
48. **Jung M, Grunberg S, Timblin C, Buder-Hoffman S, Vacek P, Taatjes DJ, Mossman BT** 2004 Paclitaxel and vinorelbine cause synergistic increases in apoptosis but not in microtubular disruption in human lung adenocarcinoma cells (A-549). Histochem Cell Biol 121:115–121
49. **Basu R, Chang F** 2007 Shaping the actin cytoskeleton using microtubule tips. Curr Opin Cell Biol 19:88–94
50. **Kline-Smith SL, Walczak CE** 2004 Mitotic spindle assembly and chromosome segregation: refocusing on microtubule dynamics. Mol Cell 15:317–327
51. **Goodman B, Zheng Y** 2006 Mitotic spindle morphogenesis: Ran on the microtubule cytoskeleton and beyond. Biochem Soc Trans 34(Pt 5):716–721

52. **O'Connell CB, Khodjakov AL** 2007 Cooperative mechanisms of mitotic spindle formation. J Cell Sci 120:1717–1722
53. **Roussel E, Belanger MM, Couet J** 2004 G2/M blockade by paclitaxel induces caveolin-1 expression in A549 lung cancer cells: caveolin-1 as a marker of cytotoxicity. Anticancer Drugs 15:961–967
54. **Sudo T, Nitta M, Saya H, Ueno NT** 2004 Dependence of paclitaxel sensitivity on a functional spindle assembly checkpoint. Cancer Res 64:2502–2508
55. **Cuttitta F, Pio R, Garayoa M, Zudaire E, Julian M, Elsasser TH, Montuenga LM, Martinez A** 2002 Adrenomedullin functions as an important tumor survival factor in human carcinogenesis. Microsc Res Tech 57:110–119
56. **Martinez A, Oh HR, Unsworth EJ, Bregonzio C, Saavedra JM, Stetler-Stevenson WG, Cuttitta F** 2004 Matrix metalloproteinase-2 cleavage of adrenomedullin produces a vasoconstrictor out of a vasodilator. Biochem J 383(Pt 3):413–418
57. **Miller MJ, Martinez A, Unsworth EJ, Thiele CJ, Moody TW, Elsasser T, Cuttitta F** 1996 Adrenomedullin expression in human tumor cell lines. Its potential role as an autocrine growth factor. J Biol Chem 271:23345–23351
58. **Ma Y, Croxton R, Moorer Jr RL, Cress WD** 2002 Identification of novel E2F1-regulated genes by microarray. Arch Biochem Biophys 399:212–224
59. **Hegedus B, Zach J, Czirok A, Lovey J, Vicsek T** 2004 Irradiation and Taxol treatment result in non-monotonous, dose-dependent changes in the motility of glioblastoma cells. J Neurooncol 67:147–157
60. **Glynn SA, Gammell P, Heenan M, O'Connor R, Liang Y, Keenan J, Clynes M** 2004 A new superinvasive in vitro phenotype induced by selection of human breast carcinoma cells with the chemotherapeutic drugs paclitaxel and doxorubicin. Br J Cancer 91:1800–1807
61. **Dallegri F, Lanzi G, Patrone F** 1980 Evidence for a reversible functional state of neutrophil chemotactic deactivation. Int Arch Allergy Appl Immunol 63: 330–337
62. **Kim W, Moon SO, Sung MJ, Kim SH, Lee S, So JN, Park SK** 2003 Angiogenic role of adrenomedullin through activation of Akt, mitogen-activated protein kinase, and focal adhesion kinase in endothelial cells. FASEB J 17:1937–1939
63. **Yang JH, Jiang W, Pan CS, Qi YF, Wu QZ, Pang YZ, Tang CS** 2004 Effects of adrenomedullin on cell proliferation in rat adventitia induced by lysophosphatidic acid. Regul Pept 121:49–56
64. **Niu P, Shindo T, Iwata H, Iimuro S, Takeda N, Zhang Y, Ebihara A, Suematsu Y, Kangawa K, Hirata Y, Nagai R** 2004 Protective effects of endogenous adrenomedullin on cardiac hypertrophy, fibrosis, and renal damage. Circulation 109:1789–1794
65. **Ichikawa-Shindo Y, Sakurai T, Kamiyoshi A, Kawate H, Iinuma N, Yoshizawa T, Koyama T, Fukuchi J, Iimuro S, Moriyama N, Kawakami H, Murata T, Kangawa K, Nagai R, Shindo T** 2008 The GPCR modulator protein RAMP2 is essential for angiogenesis and vascular integrity. J Clin Invest 118:29–39
66. **Fritz-Six KL, Dunworth WP, Li M, Caron KM** 2008 Adrenomedullin signaling is necessary for murine lymphatic vascular development. J Clin Invest 118: 40–50
67. **Yoshida N, Haga K, Haga T** 2003 Identification of sites of phosphorylation by G-protein-coupled receptor kinase 2 in β-tubulin. Eur J Biochem 270:1154–1163

Endocrinology **is published monthly by The Endocrine Society (http://www.endo-society.org), the foremost professional society serving the endocrine community.**